REMPI as a tool for studies of OH radicals in catalytic reactions

A.-P. Elg, M. Andersson, A. Rosén

Department of Physics, Göteborg University and Chalmers University of Technology, S-412 96 Göteborg, Sweden
(Fax: +46-31/7723496, E-mail: f3cae@fy.chalmers.se, f3car@fy.chalmers.se)

Abstract. The catalytic reaction $H_2 + \frac{1}{2}O_2 \rightarrow H_2O$ on poly-crystalline Pt foils has been studied by detection of desorbing OH radicals using the Resonance Enhanced Multiphoton Ionization, REMPI, technique. The measurements were performed at catalyst temperatures of 1000–1400 K and a total pressure below 10^{-4} mbar. The studies of OH desorption by REMPI were achieved using a two-photon excitation $D^2\Sigma^- - X^2\Pi$ (1–0), followed by one-photon ionization. The ions were detected in a time-of-flight mass spectrometer, TOF-MS, in order to avoid interference from non-resonantly ionized molecules. By applying TOF-MS, a simultaneous non-resonant ionization and detection of H_2, O_2 and H_2O was achieved. Recorded REMPI spectra were compared with spectra simulated using known molecular constants. The kinetics of the reaction derived from the measurements were compared with what was obtained in earlier LIF detection of OH, performed at higher total reactant pressure using the A–X transition. REMPI TOF-MS is shown to be a complement to LIF for reaction studies below 5×10^{-4} mbar total pressure, where LIF is too insensitive for quantification. The reaction kinetics was found to be in agreement with a theoretic model and previous LIF studies.

PACS: 33.80K, 07.75, 82.65J

Catalytic reactions have been the subject of extensive studies during recent decades. Surface processes have been analysed by surface sensitive techniques to probe species on the surfaces [1], or by detection of desorbed species in the gas phase [2]. In the latter case, desorbed species are often studied with thermal desorption spectroscopy (TDS) combined with mass spectrometry [3], which gives information about the coverage and adsorption energy, or in more advanced experiments, the velocity and angular distributions. In molecular beam and/or scattering experiments, molecules can be prepared in certain vibrational and rotational states before being scattered at the surface. State-sensitive, often laser-based techniques, can then be used to probe the states of the scattered molecules. These scattering experiments have pro-

vided valuable information about the kinetics and dynamics of desorption processes [4].

Access to tunable, narrow-linewidth dye lasers has improved the ability to detect desorbed species, either products or intermediates, at very low concentrations, and allowed the investigation of the kinetics and dynamics of surface and gas-phase reactions [2]. Laser-Induced Fluorescence (LIF) and Resonantly Enhanced Multiphoton Ionization (REMPI) are two techniques with the ability to provide information about the energy distribution between vibrational and/or rotational states of molecules [2, 5].

In many LIF studies, resonant one-photon excitation is used, and therefore the interpretation of the spectra is relatively straightforward. With REMPI, the situation is more complicated due to the multiphoton transitions. LIF spectra are directly interpretable concerning state distributions, while REMPI may suffer from uncertainties in the ionization step and the value of matrix elements of the multiphoton excitation, including competing processes such as relaxation, pre-dissociation and optical balance [6]. The strength of the REMPI technique lies in its high sensitivity, often two or three orders of magnitude better than LIF [5], and the ability to detect molecules with high excitation energies, such as CO and N_2. REMPI has earlier been used to detect radicals such as NO [7] and OH [8], and has also been used as a probe of partial CO pressures down to 10^{-12} mbar [9].
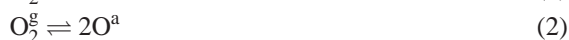
Following the pioneering work by Lin and co-workers [10, 11], the LIF technique has been used extensively in our group for studies of the OH intermediate in the catalytic formation of water from H_2 and O_2 on polycrystalline Pt [12–14], and in the decomposition of water in the presence of O_2 or H_2 [15]. These investigations of OH desorbing from a hot catalyst, have recently been extended to studies of the formation and decomposition of water on Pt(111) [16, 17], and to studies of flow conditions in the region outside the catalyst for the reactants and the diffusion of desorbed OH at pressures up to 15 mbar [18–20].

In this work, we have studied OH radicals produced in the catalytic formation of water from O_2 and H_2 on polycrystalline Pt at total pressures in the range of $10^{-7} \leq p \leq 5 \times 10^{-4}$ mbar. We detected the desorbed OH radicals with REMPI com-

bined with time-of-flight mass spectrometry (TOF-MS), and compared the results with LIF measurements, performed in earlier works at higher pressures [21], and a theoretic kinetic model of the catalytic reaction [22]. We have also analysed how the REMPI detection of OH desorbing from the surface is influenced by a large H_2O background.

1 Catalytic water formation

In previous investigations of the catalytic water formation, the mean-field approximation has successfully been used to model the reaction kinetics. This approach is also adopted here to describe the oxidation of hydrogen on Pt, leading to the formation of H_2O, and is given by [22–24]:

$$H_2^g \rightleftharpoons 2H^a \tag{1}$$
$$O_2^g \rightleftharpoons 2O^a \tag{2}$$
$$O^a + H^a \rightleftharpoons OH^a \tag{3}$$
$$OH^a + H^a \rightleftharpoons H_2O^a \tag{4}$$
$$OH^a + OH^a \rightleftharpoons H_2O^a + O^a \tag{5}$$
$$H_2O^a \rightleftharpoons H_2O^g \tag{6}$$

where the superscripts a and g denote "adsorbed" and "gas phase", respectively. Within this scheme, H_2O can be formed via two possible routes (4) and (5) of which (4) has been found to be dominant at high temperatures. At high surface temperatures, i.e. $T_s > 900\,K$ the intermediate OH desorb

$$OH^a \rightarrow OH^g \tag{7}$$

This is a minority route for consumption of adsorbed OH, because of the high activation energy for OH desorption [13], and it has minor influence on the overall reaction except at highly elevated temperatures, i.e. $T > 1400\,K$. However, the desorption rate is sufficient for efficient monitoring of the reaction intermediate with REMPI or LIF techniques. By probing the desorption rate of OH with either REMPI or LIF as a function of surface temperature, reactant pressure or gas mixture, one can measure the relative OH coverage and draw conclusions regarding the reaction kinetics on the surface. The advantage of using REMPI lies in the possibility to perform simultaneous measurements of OH and H_2O, compared to the earlier used combination of LIF and microcalorimetry.

2 Experimental techniques and procedures

2.1 Vacuum system and detection techniques

An overview of the experimental set-up constructed for the REMPI and LIF measurements is shown in Fig. 1. The vacuum chamber consists of two sections separated by a gate valve: one section for the laser excitation/ionization and a separate drift chamber with an ion detector for TOF-MS. The sections are differentially pumped by two turbomolecular pumps (240 l/s), which provides a pressure ratio during reaction of 30 : 1 between the ionization and detection chamber, and thereby increasing the highest operable pressure in the ionization chamber. The laser excitation/ionization takes place between two plates in the ion optics of the TOF-MS, as shown in Fig. 2.

The ion optics consist of an acceleration stage and an ion lens in front of the entrance to the field-free region. The two-field acceleration configuration is used to enhance the mass resolution [25]. The Einzel lens is used for focusing of the ion beam and thus enhance the signal at the detector. The flight path is about 0.5 m, and the ion-optic voltages were optimized to achieve a high detection efficiency combined with a sufficient mass resolution $m/\Delta m = 80$. We used dual microchannel plates (MCP, Galileo 3025) as ion detectors.

In order to be able to investigate the internal energy distribution of the desorbed molecules, before they undergo any gas-phase interactions, the excitation/ionization zone has to be kept close to the catalytic surface. Therefore, the catalyst, a polycrystalline Pt foil, 5 by 30 mm and 25 μm thick, is stretched and moved into an opening in the repeller plate of the ion optics using an xyz manipulator. The Pt foil is resistively heated by a direct current to temperatures between 1000 and 1400 K, determined by a four point resistance measurement [21]. The reactants are via UHV leak valves admitted into the ionization chamber, in which the total pressure is monitored by a BA-gauge previously calibrated against a capacitance gauge in the $p = 10^{-5}–10^{-4}$ mbar range. The H_2/O_2 gas mixture is monitored by a quadrupole mass spectrometer (Balzers QMS2OO). The total reactant pressures are $10^{-7} \leq p \leq 5 \times 10^{-4}$ mbar for REMPI and $p \geq 5 \times 10^{-4}$ mbar for LIF.

In order to cover a broader pressure range, the set-up is also equipped with a LIF detection using imaging optics and a photomultiplier tube (PMT, EMI-9558QB) as a detector mounted vertically. With this set-up, the species can now either be detected by imaging of fluorescence light (LIF) from a point about 2 mm in front of the catalyst surface or ionized with REMPI, accelerated by a static field into the TOF-MS and detected by the MCP. Since a TOF-MS is used for mass selection, more than one mass can be monitored simultaneously. In this way, we ionize the less abundant intermediate OH resonantly and the reaction product H_2O non-resonantly.

The signal from the MCP detector was amplified in a fast amplifier (Stanford Research Systems SR440), after which mass spectra were obtained by averaging on a digital storage oscilloscope (LeCroy 9400 or 9360). Measurements of the time-evolution of the signal for a specific ion, e.g. while scanning the laser wavelength, were performed by integration of the signal in one or several gated boxcars (SR250), i.e. several mass numbers could be recorded simultaneously. The signal from the PMT used in the LIF detection was also integrated in a gated boxcar. All outputs from the boxcars, the signal from the monitor output of the pressure gauge control unit and the sample temperature were digitized in an 8-channel A/D converter (SR245). The data were transferred via a GPIB interface and stored in an IBM PC-compatible computer at the repetition rate of the laser.

2.2 Laser spectroscopy of OH

A schematic energy level diagram for the OH molecule, with the transitions used in the LIF and REMPI measurements indicated, is presented in Fig. 3. The parameters for the $X^2\Pi$ ground state and the first excited state, $A^2\Sigma^+$, are well known in the literature [26] and have been utilized in many LIF studies of OH [10, 21]. The $B^2\Sigma^+$, and the $C^2\Sigma^+$ states both have large internuclear distances, 1.87 and 2.05 Å,
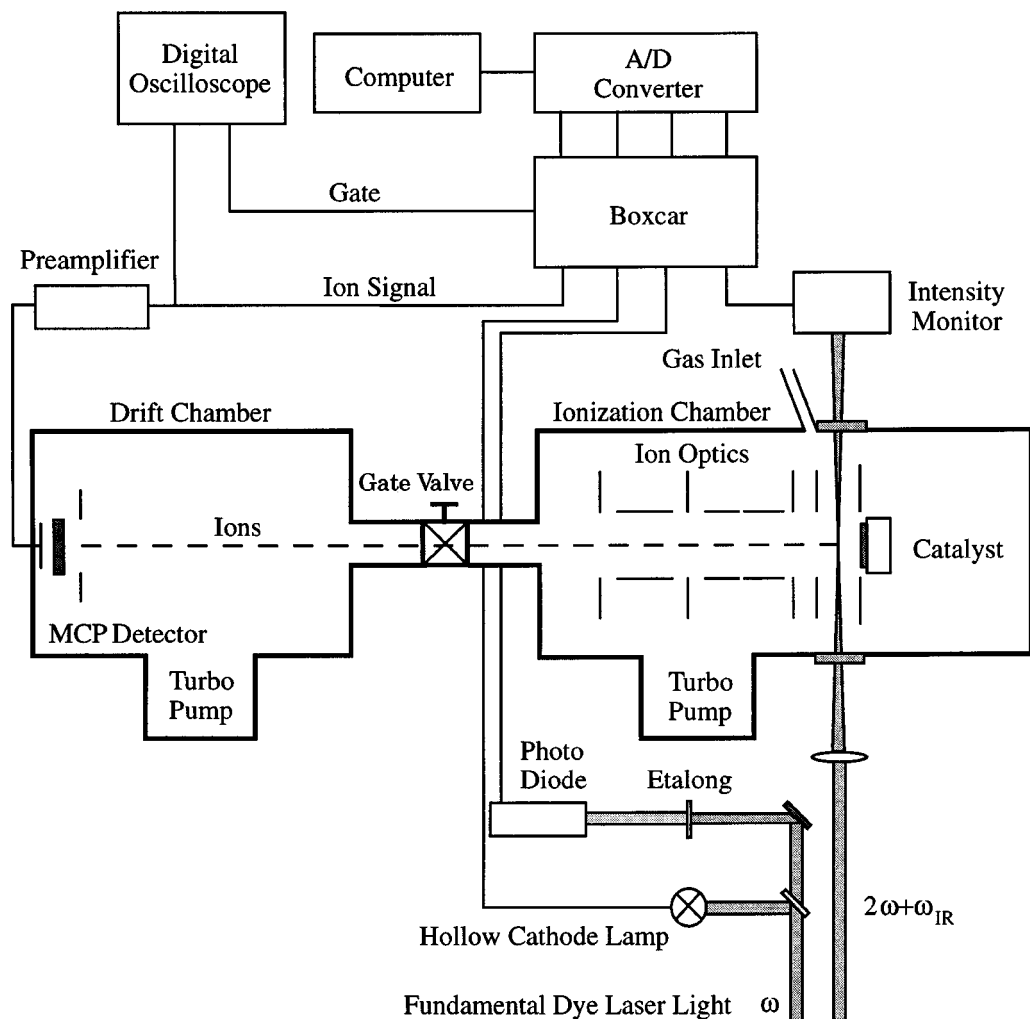
Fig. 1. An overview of the experimental set-up. The UV excitation light path is marked $2\omega + \omega_{IR}$ and the fundamental dye laser light is marked ω. The signal paths are indicated by solid lines, and the ion flight path in the vacuum chamber by a broken line. A photo multiplier tube and imaging optics for LIF detection is mounted vertically (not included in the figure), perpendicular to both the ion flight path and the laser beam

respectively [26], compared with the ground state distance of 0.96 Å. The Franck–Condon factors are relatively small for transitions to these states from the ground state. However, the (8,0) band has been detected in the $B^2\Sigma^+ - X^2\Pi$ transition by Sappey et al. [27]. A state with an internuclear distance similar to the ground state is the $D^2\Sigma^-$-state, which has been studied in OH, produced by laser induced dissociation of H_2O_2 [8] and in discharge experiments [28]. Two bands, (0,0) and (1,0), were observed in the former study [8], using $2 + 1$ photon REMPI at 244–247 nm and 236–239 nm, respectively.

In these experiments a Nd:YAG-laser-pumped dye laser, (Continuum YG671C-10 and TDL 51) with a repetition rate of 10 Hz and a doubling and mixing option, was used for the excitation and for resonant as well as non-resonant ionization. The laser wavelengths 236–239 nm for the $X^3\Sigma^-$(ion)$-D^2\Sigma^- - X^2\Pi$ transition were obtained by mixing the fundamental of the Nd:YAG laser (1064 nm) with the frequency-doubled output of the dye laser (303–308 nm). The appropriate dye to generate 236–239 nm light is Rh640, and the frequency-doubled light of this dye gives the appropriate wavelength for the (0,0) band in the $A^2\Sigma^+ - X^2\Pi$ transition (306–308 nm), which is a transition well suited for LIF studies of OH. The energy in the mixed output of the dye laser was about 3 mJ/pulse.

By splitting the fundamental of the dye laser into two beams, a relative wavelength reference was obtained by monitoring a part of the fringes from a Fabry–Perot etalon with a photodiode, and an absolute reference was recorded opto-galvanically from a Li hollow cathode lamp filled with Ne. Three separate Ne lines, at 607.60194, 609.78507 and 614.47628 nm [29] (vacuum wavelengths), were used for wavelength calibration, giving an accurate control of the dye laser wavelength. Thus, the uncertainty in the wavelength is given by the uncertainty of the fundamental of the Nd:YAG laser, since the light used for REMPI is generated by mix-
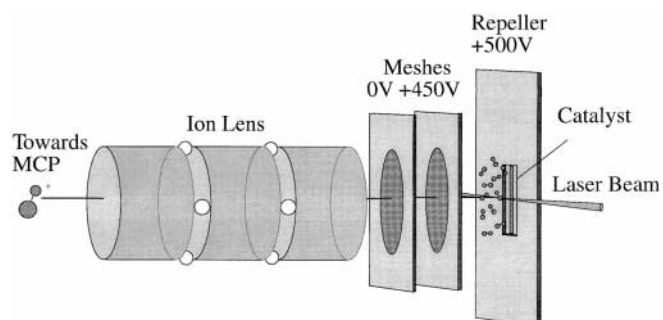

Fig. 2. A schematic of the catalyst in the ion optics

ing the uncalibrated fundamental of the Nd:YAG, with the calibrated frequency doubled dye laser light.

The bandwidth (FWHM) of the Nd:YAG laser was specified by the manufacturer to be $\leq 0.05\,\mathrm{cm}^{-1}$ and the width of the fundamental of the dye laser $\leq 0.08\,\mathrm{cm}^{-1}$. However, by measuring the width of the Ne lines the actual dye laser width was estimated to $\leq 0.26\,\mathrm{cm}^{-1}$. We can not exclude saturation of the Ne lines but it gives us an upper limit of the actual width. This gives a width of the mixed light of $\leq 0.37\,\mathrm{cm}^{-1}$ at 236–239 nm and the same for the frequency doubled light at 306–308 nm.

After passing a Glan–Taylor polarizer, the UV laser light was focused to obtain the high intensities required for the two-photon excitations in the REMPI experiments. By monitoring the laser intensities with a pyroelectric detector, the position of the focusing lens was adjusted so that the ion signal was as nearly as possible proportional to I^3. In this case, the highest dependence that we could obtain was $I^{2.7}$, a condition which was maintained during the experiments. This power dependence has previously been observed and interpreted as a focusing effect [9, 30, 31]. In order to perform an analysis of the ground state population in OH it is important not to saturate the excitation step, because of the difference in the relative transition probabilities between different rotational quantum numbers and branches.

3 Results and discussion

REMPI was used to probe the water formation reaction for a total pressure of O_2 and H_2 between 10^{-7} and 5×10^{-4} mbar, at different reactant mixtures and surface temperatures. Since photon detection is less sensitive than ion detection, measurements of the OH yield by LIF had to be performed above 5×10^{-3} mbar for an acceptable signal to noise ratio. The LIF measurements carried out in this set-up served as a reference to earlier measurements [14, 16] and gave comparable results. LIF data will therefore not be displayed or discussed further
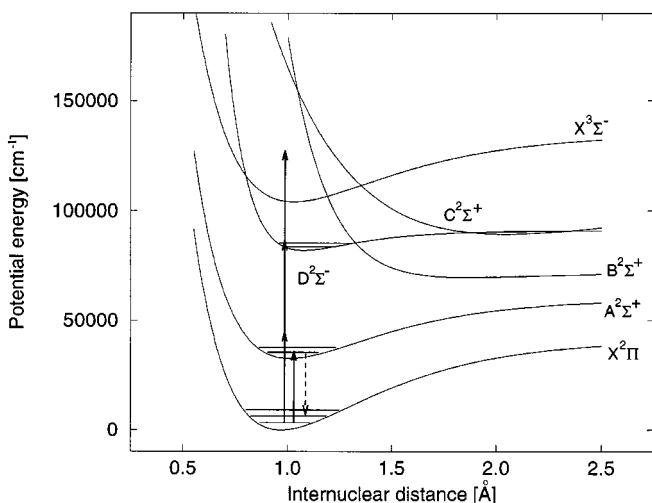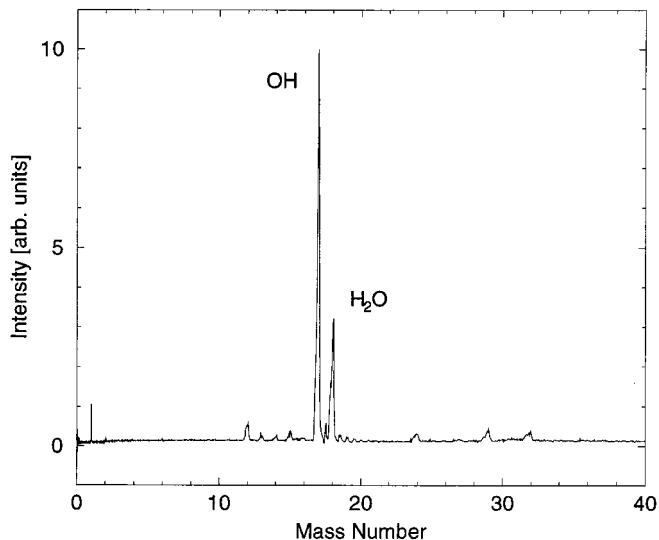

Fig. 4. A mass spectrum recorded at $p = 5 \times 10^{-5}$ mbar with the laser tuned on a OH resonance at $T_{\mathrm{sample}} = 1300$ K. The OH peak is clearly dominating the H_2O peak due to the resonant ionization

in this paper, instead the discussion will be focused on the results of REMPI measurements.

A time-of-flight mass spectrum measured at a sample temperature of 1300 K, a total pressure of 5×10^{-5} mbar and a partial H_2 pressure α ($\alpha = p_{H_2}/(p_{H_2} + p_{O_2})$) of 16% is shown in Fig. 4. The resolution of the mass spectrometer ($m/\Delta m = 80$) is sufficient to separate the OH signal from the H_2O signal. In the mass spectrum shown in Fig. 4 the reaction product H_2O gives a relatively strong signal, and wavelength scans show a weakly resonant behaviour. The other peaks originate from fragmented hydrocarbons, present in the residual gas, and weak H_2 and O_2 signals. The detection limit of OH in this experiment was reached at a total reactant pressure of 10^{-7} mbar at a surface temperature of 1380 K.

It is important to minimize the production of OH by laser-induced dissociation of H_2O, which would make any interpretation of the OH desorption rate ambiguous. To check for this, the surface temperature was lowered from 1300 K, where the OH desorption rate is high, down to 900 K (Fig. 5), a temperature at which the water production is high but the rate of OH desorption is negligible [21]. Model calculations indicate an about two orders of magnitude higher yield of H_2O than OH at 1300 K, and four orders of magnitude at 900 K. A tiny OH signal can be seen in the mass spectrum of Fig. 5 at 900 K, and this laser-induced water dissociation is found to be proportional to the water signal and the OH signal is corrected accordingly.

A wavelength scan from 236 to 238 nm with REMPI $2 + 1$ detection at a pressure of 6×10^{-5} mbar and $\alpha = 10\%$ is shown in Fig. 6, together with a simulated spectrum. The REMPI spectrum has similarities with the spectrum recorded by Collard et al. [8] for OH produced by the dissociation of H_2O_2. The spectral resolution is broad, $2.2\,\mathrm{cm}^{-1}$, compared to the expected width of a two photon excitation $\leq 0.52\,\mathrm{cm}^{-1}$, using the laser line width $\leq 0.37\,\mathrm{cm}^{-1}$ given earlier. Collard et al. related their spectral resolution, $3\,\mathrm{cm}^{-1}$, to a combination of the laser width and Doppler broadening. Doppler broadening accounts for $\sim 1.54\,\mathrm{cm}^{-1}$, assuming a thermal distribution of the desorbing OH molecules of 80% of the surface tempera-

Fig. 3. The energy level diagram of the OH molecule with the excitations, ionization and fluorescence indicated as arrows. Only the $X^3\Sigma^-$ state belongs to OH^+. In the LIF experiment we have excitation and fluorescence via the $A^2\Sigma^+$-state, and REMPI is performed via the $D^2\Sigma^-$-state

ture, which adds up to $1.62\,\mathrm{cm^{-1}}$ when combined with the laser line width of 2 photon resonant excitation. This estimate is the upper limit, since the OH radicals are probably cosine distributed around the surface normal, which is perpendicular to the laser beam.

By using the parameters given by Collard et al. [8], the theoretical REMPI spectrum gives general agreement with our experimental spectrum. However, a careful comparison between the simulated and the experimental spectra shows differences in temperature between the branches and missing peaks. The theoretical spectrum gives best agreement with the experimental spectrum when simulated using Hönl–London factors and a Boltzmann distribution of $\sim 800\,\mathrm{K}$. This is surprising since the expected temperature of OH in thermal equilibrium with the surface is 80% of the surface temperature [13]. In an earlier LIF experiment, using the A–X transition of OH and OD, a strong coupling between the angular part and the radial part of the wave functions was observed and compared with calculations [32]. Such a coupling is very likely also present for the D–X transition, and if this is the case, the simulation procedure will underestimate the rotational temperature. For a more detailed interpretation of the spectra, including determinations of state distributions, a better resolution or more precise parameters for the $D^2\Sigma^-$ state would be useful, but more important is a better estimation of transition probabilities.

Information about the rotational distributions can easily be extracted using LIF in the X–A transition. However, because of collisions affecting the ion detection at pressures suitable for LIF, and the lesser sensitivity in photon detection, we can not simultaneously use both methods. An extrapolation of a distribution in pressure, based on LIF measurements, is not reliable since the desorption mechanism is unknown and may be affected by lateral interactions on the surface due to the higher coverages at 5×10^{-3} mbar. Based on uncertainties about the desorption mechanism and unknown transition probabilities, conclusions regarding rotational distributions and ionization probabilities can not be made at the present state.
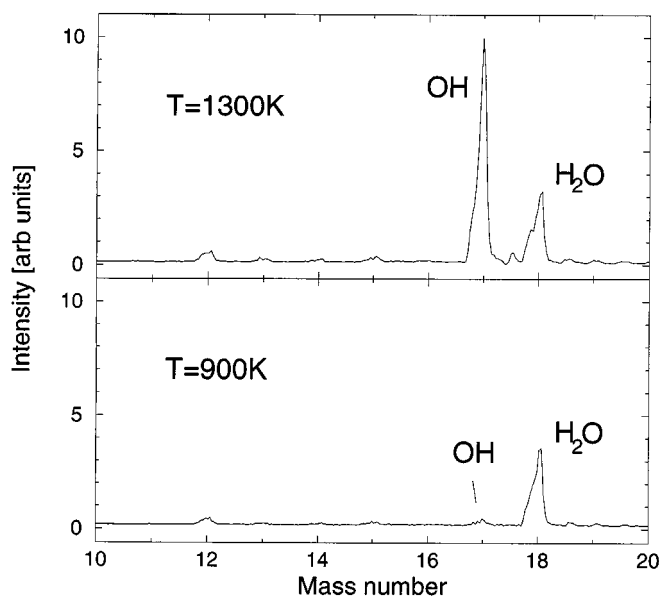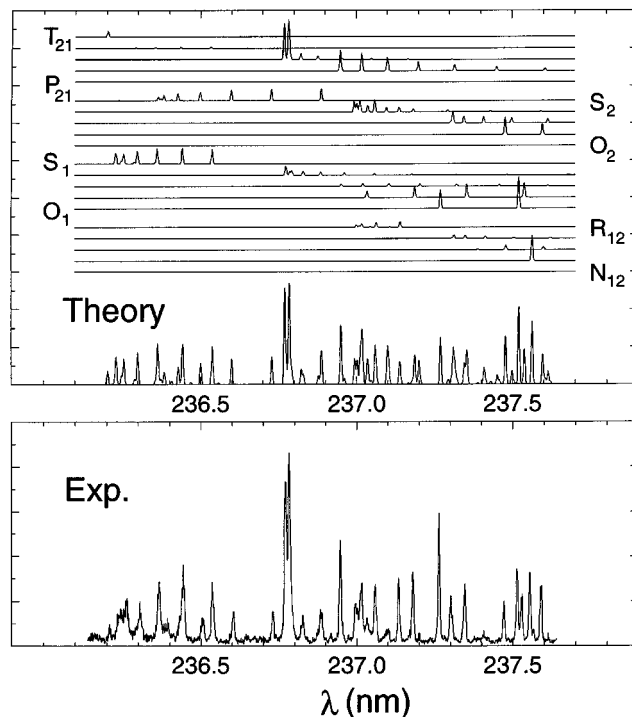

Fig. 6. A wavelength scan obtained with REMPI (bottom) for $T_{sample} = 1380\,\mathrm{K}$ and $p = 6 \times 10^{-5}$ mbar, and a simulated spectrum (top) assuming a Boltzmann distribution with $T = 800\,\mathrm{K}$. The branches in the simulation are plotted separately above the spectrum, from the bottom to the top in the order N_{12}, O_{12}, P_{12}, Q_{12}, R_{12}; O_1, P_1, Q_1, R_1, S_1; O_2, P_2, Q_2, R_2, S_2; P_{21}, Q_{21}, R_{21}, S_{21}, and T_{21}. The satellite branches are present, even though they are weaker, which can be observed e.g. at 236.2 nm with $T_{21}(1)$

However, our ambition of the work presented here is to show that OH radicals, desorbed from a catalyst surface, can be detected with REMPI and be used for investigation of catalytic reactions. The higher sensitivity of REMPI compared to LIF should allow for studies of reactions at much lower pressures than in earlier studies. Because of uncertainties in the rotational state distributions we have here limited the comparison to analysis of the yield of OH. At constant surface temperature, one can assume that the intensity of one resonance peak is proportional to the total amount of desorbed species and, thus, it is possible to study the OH desorption rate e.g. as a function of partial and total pressure.

In earlier LIF studies [14, 16] much information was gained by comparing the OH yield with measurements of the H_2O production rate using microcalorimetry. The lower reactant pressure used in this work does not allow for this method to detect water. Instead, with TOF-MS the more abundant H_2O molecules may be detected by non-resonant ionization simultaneously with REMPI of the much less abundant OH intermediate. As a demonstration of this, a measurement of the rates of OH and H_2O desorption as a function of the partial H_2 pressure α, at a constant total pressure of 5×10^{-5} mbar, is given in Fig. 7, recorded using the $O_1(3)$ peak at 237.51 nm, according to the experimental spectrum in Fig. 6. The results shown in Fig. 7 are in good agreement with results from LIF studies at higher pressures [16], with shapes well described by the kinetic model [22] (solid lines). The experimental data are also in agreement with the model with respect to an observed shift of the maxima of OH and H_2O yield. The maximum desorption rates for OH and H_2O are shifted from $\alpha = 0.12$ and

Fig. 5. Two mass spectra obtained at $T_{sample} = 1300\,\mathrm{K}$ (top) and at $T_{sample} = 900\,\mathrm{K}$ (bottom), and a total reactant pressure of $p = 5 \times 10^{-5}$ mbar The laser was tuned on a resonance in OH and 1000 shots were averaged
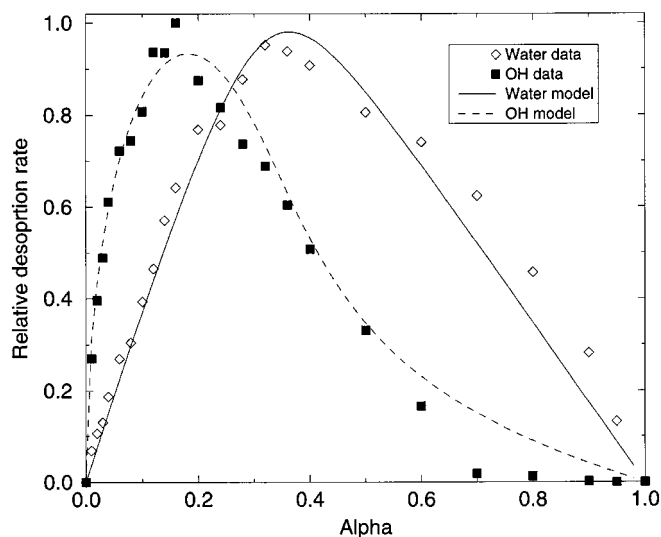
Fig. 7. A plot of the OH and H$_2$O signals (normalized) as functions of the partial pressure of H$_2$, $\alpha = p_{H_2}/(p_{H_2} + p_{O_2})$, at a total pressure of 5×10^{-5} mbar and a surface temperature of 1200 K. The solid and dashed lines are from calculations using the kinetic model

0.25 at 0.13 mbar total reactant pressure, measured in earlier studies with LIF [21], to $\alpha = 0.18$ and 0.36 at 5×10^{-5} mbar in this REMPI study (Fig. 7). The hydrogen rich part of the data differs from the model, but this difference has earlier been observed also in LIF experiments at higher pressures [16]. Further exploration of the detailed reaction kinetics is beyond the scope here, and will be further discussed elsewhere [33].

4 Conclusions

REMPI TOF-MS is a suitable technique for sensitive measurements of minority species, avoiding interference from majority species, e.g. OH in an H$_2$O atmosphere during the catalytic oxidation of hydrogen on Pt. H$_2$O and OH can be detected simultaneously, and provide information on the kinetics of the surface reactions. The technique is limited to measurements at reactant pressures below 5×10^{-4} mbar by the mass-spectrometric detection, but allows for efficient detection above a total reactant pressure of 5×10^{-7} mbar. REMPI TOF-MS is clearly a complement to LIF, being applicable at lower pressures which allows for comparison with methods in situ probing the coverages on the surface, e.g. second harmonic generation, SHG, [34, 35].

Given the fact that simultaneous quantitative measurements of LIF and REMPI are not possible for this system, that the two-photon transition D–X (1,0) transition probabilities may be coupled to the radial part combined with uncertainties in the ionization efficiencies, an extraction of rotational state distributions is difficult. On the other hand, at constant surface temperature and at constant total pressure, the OH desorption

rate as a function of α has been found to be in agreement with previous investigations.

References

1. P.R. Norton: in *The Chemical Physics of Solid Surfaces and Heterogenous Catalysis, Vol. IV*, ed. by D.A. King, D.P. Woodruff (Elsevier, Amsterdam 1982) p.27
2. M.C. Lin, G. Ertl: Ann. Rev. Phys. Chem. **37**, 587 (1986)
3. G. Comsa, R. David: Surf. Sci. Reports **5**, 145 (1985)
4. J.A. Barker, D.J. Auerbach: Surf. Sci. Reports **4**, 1 (1985)
5. H. Zacharias: Int. J. Mod. Phys. B **4**, 45 (1990)
6. J.J. Wynne: Phys. Rev. Lett. **52**, 751 (1984)
7. D.J. Jacobs, R.J. Madix, R.N. Zare: J. Chem. Phys. **85**, 5469 (1986)
8. M. Collard, P. Kerwin, A. Hodgson: Chem. Phys. Lett. **179**, 422 (1991)
9. J.P. Looney, J.E. Harrington, K.C. Smith, T.R. O'Brian, T.B. Lucatorto: J. Vac. Sci. Technol. A **11**, 3111 (1993)
10. L.D. Talley, W.A. Sanders, D.J. Bogan, M.C. Lin: J. Chem. Phys. **75**, 3107 (1981)
11. L.D. Talley, W.A. Sanders, D.J. Bogan, M.C. Lin: Chem. Phys. Lett. **78**, 500 (1981)
12. S. Ljungström, J. Hall, B. Kasemo, A. Rosén, T. Wahnström: J. Catal. **107**, 548 (1987)
13. T. Wahnström, E. Fridell, S. Ljungström, B. Hellsing, B. Kasemo, A. Rosén: Surf. Sci. **223**, L905 (1989)
14. T. Wahnström, S. Ljungström, A. Rosén, B. Kasemo: Surf. Sci. **234**, 439 (1990)
15. E. Fridell, A. Rosén, B. Kasemo: Langmuir **10**, 699 (1994)
16. E. Fridell, A.P. Elg, A. Rosén, B. Kasemo: J. Chem. Phys **102**, 5827 (1995)
17. E. Fridell, PhD thesis, University of Göteborg (1993)
18. E. Fridell, U. Westblom, M. Aldén, A. Rosén: J. Catal. **128**, 92 (1991)
19. F. Gudmundson, F. Fridell, A. Rosén, B. Kasemo: J. Phys. Chem. **97**, 12828 (1993)
20. F. Gudmundson, F. Behrendt, A. Rosén: in *Laser techniqnes for surface science II*, Proc. SPIE 2547, ed. by J.M. Hicks, W. Ho, H.L. Dai (1995), p.52
21. S. Ljungström, B. Kasemo, A. Rosén, T. Wahnström, Fridell: Surf. Sci. **216**, 63 (1989)
22. B. Hellsing, B. Kasemo, V.P. Zhdanov: J. Catal. **132**, 210 (1991)
23. B. Hellsing, B. Kasemo, S. Ljungström, A. Rosén, T. Wahnström: Surf. Sci. **189/190**, 851 (1987)
24. V.P. Zhdanov: Surf. Sci. **296**, 261 (1993)
25. W.C. Wiley, H. McLaren: Rev. Sci. Instr. **26**, 1150 (1955)
26. K.P. Huber, G. Hertzberg: *Molecular Spectca and Molecular Structure, IV. Constants of Diatomic Molecules* (Van Nostrand Reinhold, New York 1979)
27. A.D. Sappey, D.R. Crosley, R.A. Copeland: J. Chem. Phys. **90**, 3484 (1989)
28. A.E. Douglas: Can. J. Phys. **52**, 318 (1974)
29. V. Kaufman, B. Edlén: J. Phys. Chem. Ref. Data **3**, 827 (1974)
30. D.R. Crosley, G.P. Smith: J. Chem. Phys. **79**, 4764 (1983)
31. S.H. Lin, Y. Fujimura, H.J. Neusser, E.W. Schlag: *Multiphoton Spectroscopy of Molecules* (Academic Press, London 1984)
32. I.L. Chidsey, D.R. Crosley: J. Quant. Spectrosc. Radiat. **23**, 187 (1980)
33. A.P. Elg, M. Andersson, A. Rosén, to be published
34. F. Eisert, A.P. Elg, A. Rosén: Appl. Phys A **60**, 209 (1995)
35. F. Eisert, A. Rosén: Phys. Rev. B **54**, 14061 (1996)